Inorg. Chem. **2006**, *45*, 1924–1934

Synthesis, Structures, and Magnetic Properties of Tetranuclear Cu^{II}–Ln^{III} Complexes

Jean-Pierre Costes,*,† Magali Auchel,† Françoise Dahan,† Viviane Peyrou,† Sergiu Shova,‡ and Wolfgang Wernsdorfer§

Laboratoire de Chimie de Coordination du CNRS, UPR 8241, liée par conventions à l'Université Paul Sabatier et à l'Institut National Polytechnique de Toulouse, 205 route de Narbonne, 31077 Toulouse Cedex, France, Department of Chemistry, Moldova State University, A. Mateevici str. 60, 2009 Chisinau, Moldova, and Laboratoire Louis Néel du CNRS, BP 166, 38042 Grenoble Cedex 9, France

Received April 15, 2005

The copper(II)–gadolinium(III) and copper(II)–terbium(III) complexes studied in this report derive from disymmetric trianionic ligands abbreviated H_3L^i (i = 4–6). These ligands are obtained through reaction of different aldehydes with "half-units" having an amide function, the latter resulting from the monocondensation of different diamines with phenyl 2-hydroxy-3-methoxybenzoate. Upon deprotonation, the L^i ligands (i = 4–10) possess an inner N_2O_2 coordination site with one amido, one imine, and two phenoxo functions, an outer O_2O_2 or O_2O coordination site, and an amido oxygen atom positioned out of these two sites. The trianionic character of such ligands yields original anionic complexes in the presence of copper(II) or nickel(II) ions, with a 1/1 L/M stoichiometry. The crystal and molecular structures of four complexes, two 3d (**1**, **5**) and two 3d–4f (**12**, **13**) complexes, have been determined. Complex **1** crystallizes in the monoclinic space group $C2/c$: a = 27.528(2) Å, b = 7.0944(7) Å, c = 22.914(2) Å, β = 92.130(6)°, V = 4471.9(7) Å^3, Z = 8 for $C_{21.5}H_{27}CuKN_2O_{6.5}$. Complex **5** crystallizes in the monoclinic space group $P2_1/n$ (No. 14): a = 11.0760(9) Å, b = 21.454(2) Å, c = 15.336(1) Å, β = 101.474(1)°, V = 3571.5(5) Å^3, Z = 4. Complex **12** crystallizes in the triclinic space group $P\bar{1}$ (No. 2): a = 8.682(2) Å, b = 11.848(2) Å, c = 11.928(2) Å, α = 81.77(3)°, β = 89.17(3)°, γ = 85.49(3)°, V = 1210.6(4) Å^3, Z = 2 for $C_{20}H_{22}CuN_5O_{11}Tb$. Complex **13** belongs to the monoclinic space group $C2/c$: a = 25.475(5)Å, b = 12.934(3)Å, c = 15.023(3) Å, β = 91.06(3)°, V = 4949.0(2)Å^3, Z = 8 for $C_{21}H_{25}CuN_4O_{12}Tb$. The structural determinations confirm that the dinuclear entities involved in **12** and **13** are disposed in a head-to-tail arrangement to give tetranuclear complexes in which the copper and lanthanide ions are positioned at the vertexes of a rectangle. In the $[Cu–Gd]_2$ species, there are two different ferromagnetic Cu–Gd interactions. The stronger one is supported by the double phenoxo bridge (CuO_2Gd) while the weaker one corresponds to the single amido bridge (Cu–N–C–O–Gd). Replacement of gadolinium ions with anisotropic terbium ions yields tetranuclear entities showing slow relaxation of magnetization and magnetization hysteresis. Detailed relaxation and hysteresis loop studies establish single-molecule magnet (SMM) behavior which is influenced by weak intermolecular interactions.

Introduction

Molecular structures made of 3d and 4f ions in close vicinity are still exciting. Among their potential applications, luminescent materials,[1] MOCVD precursors,[2] and near-infrared chiroptical sensors,[3] tetranuclear $[Cu-Tb]_2$ [4] and $[Mn-Dy]_2$ [5] complexes or clusters of higher nuclearity [Mn−

* To whom correspondence should be addressed. Fax: 33 (0)5 61 55 30 03. E-mail: costes@lcc-toulouse.fr.
† Laboratoire de Chimie de Coordination du CNRS.
‡ Moldova State University.
§ Laboratoire Louis Néel du CNRS.

(1) Edder, C.; Piguet, C.; Bünzli, J. C. G.; Hopfgartner, G. *Chem.—Eur. J.* **2001**, *7*, 3014.
(2) Gleizes, A.; Julve, M.; Kuzmina, N.; Alikhanyan, A.; Lloret, F.; Malkerova, I.; Sanz, J.; Senocq, F. *Eur. J. Inorg. Chem.* **1998**, 1169.
(3) Subhan, M. A.; Suzuki, T.; Kaisaki, S. *Dalton Trans.* **2002**, 1416.
(4) Osa, S.; Kido, T.; Matsumoto, N.; Re, N.; Pochaba, A.; Mrozinski, J. *J. Am. Chem. Soc.* **2004**, *126*, 420.
(5) Mishra, A.; Wernsdorfer, W.; Parsons, S.; Christou, G.; Brechin, E. K. *Chem. Commun.* **2005**, 2086.

10.1021/ic050587o CCC: $33.50
Published on Web 02/03/2006

Dy]$_6$[6] have been shown to function as "single-molecule magnets" (SMMs). Previously, strictly heterodinuclear complexes containing a 3d ion and a 4f ion have allowed the study of magnetic interactions, mainly in the cases where gadolinium was associated with a Cu^{II} ion[7,8] but also with VO^{IV},[9] Cr^{III},[3] Fe^{II},[10] Co^{II}, Co^{III},[11] and Ni^{II}.[12] These studies confirm that a large majority of the 3d Gd complexes present ferromagnetic 3d Gd interactions. So, assembling these dinuclear units in a manner which preserves the intramolecular ferromagnetic interactions and adds new intermolecular ferromagnetic interactions appears to be interesting. Such a result can be expected if the 3d ion of one unit interacts with the 4f ions of a unit in a near vicinity with, as a final result, the synthesis of high-spin polynuclear [3d−4f]$_n$ clusters. Some time ago, we have shown that disymmetric amide−imine ligands with a N_2O_2 coordination site and an outer oxygen atom yielded tetranuclear or polynuclear manganese complexes.[13] The addition of a second site able to link a 4f ion gives heterodinuclear entities that self-assemble to yield clusters of higher nuclearity. Two previous examples have been published.[14,15] Now, our aim is to use the changes induced in this type of ligand to obtain the best interaction parameters, to determine if the synthesis of complexes of different nuclearities is possible, and to observe the influence of symmetry on the magnetic properties of the resulting complexes.

Experimental Section

Materials. 1,2-Diaminoethane, 1,2-diamino-2-methylpropane, 1,3-diamino-2,2-dimethylpropane, orthovanillin, 3-methoxysalicylic acid, salicylamide, $Cu(OAc)_2{\cdot}4H_2O$, $Gd(NO_3)_3{\cdot}6H_2O$, and $Tb(NO_3)_3{\cdot}6H_2O$ (Aldrich) were used as received. High-grade solvents (2-propanol, dichloromethane, diethyl ether, acetone, ethanol, and methanol) were used for the syntheses of the ligands and complexes.

Ligands. The method used to synthesize the "half-unit" trifunctional ligands L^iH_2 ($i = 1-3$) was adapted from the process described earlier.[13] Only one example will be described in detail, as the experimental process is similar for all of the half-units.

L^1H_2. *N*-(2-Amino-2-methylpropyl)-2-hydroxy-3-methoxybenzamide. A mixture of 3-methoxysalicylic acid (1.68 g, 1×10^{-2} mol), phenol (2.82 g, 3×10^{-2} mol), and 1,3-dicyclohexylcarbodiimide (2.06 g, 1×10^{-2} mol) in THF (100 mL) was stirred for 24 h at room temperature. The solution was filtered off, and the THF was eliminated using a rotavapor. The resulting oil was poured into 2-propanol (40 mL), and 1,2-diamino-2-methylpropane (0.88 g, 1×10^{-2} mol) in 2-propanol (10 mL) was added dropwise; the mixture was refluxed for thirty minutes and then cooled to room temperature with stirring. The white precipitate which appeared upon cooling was filtered off and washed with diethyl ether. Yield: 1.82 g (61%). Anal. Calcd for $C_{12}H_{18}N_2O_3{\cdot}C_3H_8O$: C, 60.4; H, 8.8; N, 9.4. Found: C, 60.0; H, 8.5; N, 9.4. ^{1}H NMR (250 MHz, 20 °C, DMSO-d_6): δ 1.28 (s, 6H, CH_3), 3.52 (s, 2H, CH_2), 3.81 (s, 3H, CH_3), 6.42 (t, $J = 8$ Hz, 1H, C(5)*H*), 6.56 (l, 3H, NH_2 + N*H*), 6.88 (d, $J = 8$ Hz, 1H, C(4)*H*), 7.48 (td, $J = 1.5$ and 8 Hz, 1H, C(6)*H*), 11.43 (l, 1H, O*H*). 2-Propanol gives peaks at 1.16 (*C*H$_3$) and 3.89 ppm (*C*H). ^{13}C{^{1}H} NMR (62.896 MHz, 20 °C, DMSO-d_6): δ 25.6 (s, *C*H$_3$), 47.3 (s, *C*H$_2$), 52.8 (s, O*C*H$_3$), 111.1 (s, Ar*C*(4)H), 112.6 (s, Ar*C*(5)H), 117.2 (s, Ar*C*1), 121.1 (s, Ar*C*(6)H), 151.2 (s, Ar*C*(3)OMe), 158.2 (s, Ar*C*(2)OH), 169.2 (s, O*C*NH). 2-Propanol gives peaks at 25.2 (*C*H$_3$) and 62.1 ppm (*C*H). Characteristic IR absorptions (KBr): 2972, 1616, 1593, 1557, 1540, 1217 cm^{-1}.

L^2H_2. *N*-(2-Aminoethyl)-2-hydroxy-3-methoxybenzamide. This ligand was prepared as L^1H_2 with use of 1,2-diaminoethane (0.60 g, 1×10^{-2} mol) as the diamine. As the ^{1}H NMR spectrum confirms presence of a small amount of the symmetrical ligand, the addition of picric acid to a solution of the isolated precipitate in methanol (50 mL) gave a yellow precipitate that was filtered off, washed with diethyl ether, and dried. Yield: 1.3 g (30%). Anal. Calcd for $C_{16}H_{17}N_5O_{10}$: C, 43.7; H, 3.9; N, 15.9. Found: C, 43.3; H, 3.7; N, 15.9. ^{1}H NMR (250 MHz, 20 °C, DMSO-d_6): δ 3.14 (t, $J = 5.5$ Hz, 2H, CH_2NH$_3$), 3.65 (q, $J = 5.5$ Hz, 2H, CH_2NH), 3.89 (s, 3H, OCH_3), 6.95 (t, $J = 8$ Hz, 1H, C(5)*H*), 7.23 (d, $J = 8$ Hz, 1H, C(4)*H*), 7.50 (d, $J = 8$ Hz, 1H, C(6)*H*), 8.77 (s, 2H, CH_{pic}), 8.99 (t, $J = 5.5$ Hz, 1H, OCN*H*), 12.56 (s, 1H, O*H*). ^{13}C{^{1}H} NMR (62.896 MHz, 20 °C, DMSO-d_6): δ 37.0 (s, *C*H$_2$NH$_3$), 38.7 (s, *C*H$_2$NH), 55.9 (s, O*C*H$_3$), 115.0 (s, Ar*C*), 115.5 (s, Ar*C*(4)H), 118.0 (s, Ar*C*(5)H), 119.0 (s, Ar*C*(6)H), 148.5 (s, Ar*C*(4)OCH$_3$), 150.7 (s, Ar*C*(2)OH), 170.2 (s, O*C*NH). Picrate gives peaks at 125.4 and 141.9 ppm. Characteristic IR absorptions (KBr): 3427,1635, 1592, 1540, 1248 cm^{-1}.

L^3H_2. *N*-(3-Aminopropyl)-2-hydroxy-3-methoxybenzamide. The use of 2,2-dimethyl-1,3-diaminopropane (0.74 g, 1×10^{-2} mol) as the diamine and dichloromethane instead of 2-propanol yields the L^3H_2 ligand. Yield: 1.0 g (40%). Anal. Calcd for $C_{13}H_{20}N_2O_3$: C, 61.9; H, 8.0; N, 11.1. Found: C, 61.5; H, 7.8; N, 10.9. ^{1}H NMR (250 MHz, 20 °C, DMSO-d_6): δ 1.02 (s, 6H, CH_3), 2.57 (s, 2H, CH_2N), 3.29 (q, $J = 5.5$ Hz, 2H, CH_2NH), 3.75 (l, 3H, NH_2 + N*H*), 3.75 (s, 3H, CH_3), 6.57 (t, $J = 8$ Hz, 1H, C(5)*H*), 6.99 (dd, $J = 1$ and 8 Hz, 1H, C(4)*H*), 7.46 (dd, $J = 1$ and 8 Hz, 1H, C(6)*H*). ^{13}C{^{1}H} NMR (62.896 MHz, 20 °C, DMSO-d_6): δ 23.5 (s, *C*H$_3$), 35.7 (s, *C*(CH$_3$)$_2$), 46.0 (s, *C*H$_2$NH), 48.5 (s, *C*H$_2$N), 56.5 (s, O*C*H$_3$), 119.8 (s, Ar*C*), 112.0 (s, Ar*C*(4)H), 113.7 (s, Ar*C*(5)H), 116.9 (s, Ar*C*(6)H), 151.1 (s, Ar*C*(3)OMe), 158.0 (s, Ar*C*(2)OH), 168.5 (s, O*C*NH). Characteristic IR absorptions (KBr): 2964, 1615, 1586, 1537, 1214 cm^{-1}.

Cu^{II} Complexes. [L^4CuK(CH$_3$OH)](CH$_3$OH)$_{0.5}$ (1). A mixture of $L^1H_2{\cdot}C_3H_8O$ (0.30 g, 1×10^{-3} mol) and orthovanillin (0.15 g, 1×10^{-3} mol) in methanol (20 mL) was heated for 30 min and then left to cool with stirring. $Cu(OAc)_2{\cdot}H_2O$ (0.20 g, 1×10^{-3} mol) and KOH (0.17 g, 3×10^{-3} mol) were added. The solution was heated and stirred for 2 h, and then it was set aside after the addition of water (20 mL). Crystals appeared 24 h later. Yield: 0.22 g (42%). Anal. Calcd for $C_{21.5}H_{27}CuKN_2O_{6.5}$: C, 49.7; H, 5.2; N, 5.4. Found: C, 49.5; H, 5.3; N, 5.2. Characteristic IR absorptions (KBr): 1633, 1599, 1566, 1527, 1235 cm^{-1}.

(6) Zaleski, C. M.; Depperman, E. C.; Kampf, J. W.; Kirk, M. L.; Pecoraro, V. *Angew. Chem., Int. Ed.* **2004**, *43*, 3912.
(7) Benelli, C.; Gatteschi, D. *Chem. Rev.* **2002**, *102*, 2369.
(8) Sakamoto, M.; Manseki, K.; Okawa, H. *Coord. Chem. Rev.* **2001**, *219−221*, 379.
(9) Costes, J. P.; Dahan, F.; Donnadieu, B.; Garcia-Tojal, J.; Laurent, J. P. *Eur. J. Inorg. Chem.* **2001**, 363.
(10) Costes, J. P.; Clemente-Juan, J. M.; Dahan, F.; Dumestre, F.; Tuchagues, J. P. *Inorg. Chem.* **2002**, *41*, 2886.
(11) Costes, J. P.; Dahan, F.; García-Tojal, J. *Chem.−Eur. J.* **2002**, *8*, 5430.
(12) Costes, J. P.; Dahan, F.; Dupuis, A.; Laurent, J. P. *Inorg. Chem.* **1997**, *36*, 4284.
(13) Costes, J.-P.; Dahan, F.; Donnadieu, B.; Rodriguez Douton, M. J.; Fernandez Garcia, M. I.; Bousseksou, A.; Tuchagues, J.-P. *Inorg. Chem.* **2004**, *43*, 2736.
(14) (a) Kido, T.; Nagasato, S.; Sunatsuki, Y.; Matsumoto, N. *Chem. Commun.* **2000**, 2113. (b) Kido, T.; Ikuta, Y.; Sunatsuki, Y.; Ogawa, Y.; Matsumoto, N. *Inorg. Chem.* **2003**, *42*, 398.
(15) Costes, J. P.; Dahan, F. *C. R. Acad. Sci. Paris* **2001**, *4*, 97.

[L^{5}Cu](C$_5$H$_{12}$N)$_2$(C$_6$H$_2$N$_3$O$_7$) (2). A mixture of L^{2}H$_3$·picrate (0.44 g, 1 × 10^{-3} mol) and orthovanillin (0.15 g, 1 × 10^{-3} mol) in methanol (20 mL) was heated for 30 min and then left to cool with stirring. Cu(OAc)$_2$·H$_2$O (0.20 g, 1 × 10^{-3} mol) was added, followed by the addition of piperidine (0.30 g, 3.5 × 10^{-3} mol). The solution was stirred for 2 h and set aside. Concentration of the solution gave a powder that was filtered off, washed with diethyl ether, and dried. Yield: 0.40 g (49%). Anal. Calcd for C$_{34}$H$_{43}$CuN$_7$O$_{12}$: C, 50.7; H, 5.4; N, 12.2. Found: C, 50.4; H, 5.1; N, 11.8. Characteristic IR absorptions (KBr):1644, 1600, 1568, 1534, 1219 cm^{-1}.

The other copper complexes derived from the same L^{2}H$_2$ "half-unit" were obtained with a similar experimental process.

[L^{6}Cu](C$_5$H$_{12}$N)$_2$(C$_6$H$_2$N$_3$O$_7$) (3). 3-Ethoxysalicylaldehyde was used instead of orthovanillin. Yield: 0.45 g (55%). Anal. Calcd for C$_{35}$H$_{45}$CuN$_7$O$_{12}$: C, 51.3; H, 5.5; N, 12.0. Found: C, 51.1; H, 5.5; N, 11.8. Characteristic IR absorptions (KBr): 1646, 1597, 1569, 1529, 1233 cm^{-1}.

[L^{7}Cu](C$_5$H$_{12}$N)$_2$(C$_6$H$_2$N$_3$O$_7$) (4). Orthovanillin was replaced by salicylaldehyde. Yield: 0.35 g (45%). Anal. Calcd for C$_{33}$H$_{41}$CuN$_7$O$_{11}$: C, 51.1; H, 5.3; N, 12.6. Found: C, 50.8; H, 5.1; N, 12.3. Characteristic IR absorptions (KBr): 1646, 1597, 1569, 1529, 1233 cm^{-1}.

[L^{7}Ni](C$_5$H$_{12}$N)$_2$(C$_6$H$_2$N$_3$O$_7$) (5). The use of salicylaldehyde and Ni(OAc)$_2$·4H$_2$O yielded the equivalent nickel complex which was isolated as crystals. Yield: 0.38 g (49%). Anal. Calcd for C$_{33}$H$_{41}$N$_7$NiO$_{11}$: C, 51.4; H, 5.4; N, 12.7. Found: C, 51.2; H, 5.2; N, 12.5. Characteristic IR absorptions (KBr): 1627, 1598, 1533, 1235 cm^{-1}.

[L^{8}CuK](CH$_3$OH) (6). A mixture of L^{3}H$_2$ (0.25 g, 1 × 10^{-3} mol) and orthovanillin (0.15 g, 1 × 10^{-3} mol) in methanol (20 mL) was heated for thirty minutes and then left to cool with stirring. The addition of Cu(OAc)$_2$·H$_2$O (0.20 g, 1 × 10^{-3} mol) and of KOH (0.17 g, 3 × 10^{-3} mol) followed by heating and stirring for 2 h gave a precipitate after the mixture was cooled. It was filtered off, washed with methanol and diethyl ether, and dried. Yield: 0.28 g (54%). Anal. Calcd for C$_{22}$H$_{27}$CuKN$_2$O$_6$: C, 51.0; H, 5.2; N, 5.4. Found: C, 50.7; H, 5.0; N, 5.2. Characteristic IR absorptions (KBr): 1630 1566, 1538, 1219 cm^{-1}.

[L^{9}CuK](C$_3$H$_6$O) (7). The half-unit derived from the reaction of phenyl salicylate with 1,2-diamino-2-methylpropane[13] (0.21 g, 1 × 10^{-3} mol) was mixed with orthovanillin (0.15 g, 1 × 10^{-3} mol) in methanol (20 mL), heated for 30 min, and then left to cool with stirring. Cu(OAc)$_2$·H$_2$O (0.20 g, 1 × 10^{-3} mol) was added, followed by KOH (0.17 g, 3 × 10^{-3} mol). The solution was heated and stirred for 2 h and set aside. Methanol was evaporated, and the solid was dissolved in acetone. The filtered solution gave crystals 2 days later. Yield: 0.22 g (44%). Anal. Calcd for C$_{22}$H$_{25}$CuKN$_2$O$_5$: C, 52.8; H, 5.0; N, 5.6. Found: C, 52.5; H, 4.8; N, 5.4. Characteristic IR absorptions (KBr): 1707, 1600, 1563, 1528, 1253 cm^{-1}.

Heteronuclear Cu^{II}Ln^{III} Complexes. These complexes were prepared according to the general process described below.

[L^{5}CuGd(NO$_3$)$_2$]$_2$ (8). [L^{5}Cu](C$_5$H$_{12}$N)$_2$(C$_6$H$_2$N$_3$O$_7$) (0.25 g, 3.1 × 10^{-4} mol) and Gd(NO$_3$)$_3$·6H$_2$O (0.15 g, 3.3 × 10^{-4} mol) were mixed in methanol (10 mL); the mixture was stirred and heated for 15 min, and then it was cooled at room temperature. The resulting precipitate was filtered off, washed with methanol, acetone, and diethyl ether**,** and dried. Yield: 0.17 g (80%). Anal. Calcd for C$_{36}$H$_{34}$Cu$_2$Gd$_2$N$_8$O$_{22}$: C, 31.5; H, 2.5; N, 8.2. Found: C, 31.2; H, 2.3; N, 7.9. Characteristic IR absorptions (KBr): 1640, 1580, 1546, 1459, 1221 cm^{-1}.

[L^{5}CuTb(NO$_3$)$_2$]$_2$ (9). The use of Tb(NO$_3$)$_3$·6H$_2$O (0.10 g, 2.2 × 10^{-4} mol) and the same copper complex yielded the equivalent CuTb complex (77%). Anal. Calcd for C$_{36}$H$_{34}$Cu$_2$N$_8$O$_{22}$Tb$_2$: C, 31.4; H, 2.5; N, 8.1. Found: C, 31.1; H, 2.3; N, 7.8. Characteristic IR absorptions (KBr): 1639, 1580, 1547, 1459, 1222 cm^{-1}.

[L^{6}CuGd(NO$_3$)$_2$]$_2$ (10). The use of [L^{6}Cu](C$_5$H$_{12}$N)$_2$(C$_6$H$_2$N$_3$O$_7$) (0.15 g, 1.8 × 10^{-4} mol) and Gd(NO$_3$)$_3$·6H$_2$O (0.09 g, 2 × 10^{-4} mol) with the same experimental process yielded the desired product (0.10 g, 79%). Anal. Calcd for C$_{38}$H$_{38}$Cu$_2$Gd$_2$N$_8$O$_{22}$: C, 32.6; H, 2.7; N, 8.0. Found: C, 32.6; H, 2.8; N, 7.5. Characteristic IR absorptions (KBr): 1645, 1606, 1577, 1540, 1457,1222 cm^{-1}.

[L^{7}CuGd(NO$_3$)$_2$(H$_2$O)]$_2$ (11). This complex was obtained using [L^{7}Cu](C$_5$H$_{12}$N)$_2$(C$_6$H$_2$N$_3$O$_7$) (0.22 g, 2.8 × 10^{-4} mol) and Gd(NO$_3$)$_3$·6H$_2$O (0.14 g, 3 × 10^{-4} mol). Yield: (0.14 g, 71%). Anal. Calcd for C$_{34}$H$_{34}$Cu$_2$Gd$_2$N$_8$O$_{22}$: C, 30.3; H, 2.5; N, 8.3. Found: C, 29.9; H, 2.4; N, 7.9. Characteristic IR absorptions (KBr): 1640, 1620, 1599, 1584, 1541, 1447, 1250 cm^{-1}.

[L^{7}CuTb(NO$_3$)$_2$(DMF)]$_2$ (12). This complex was obtained using [L^{7}Cu](C$_5$H$_{12}$N)$_2$(C$_6$H$_2$N$_3$O$_7$) (0.17 g, 2.2 × 10^{-4} mol) and Tb(NO$_3$)$_3$·6H$_2$O (0.11 g, 2.4 × 10^{-4} mol). Crystals were obtained by slow diffusion of methanol into a DMF solution of the complex. Yield: (0.09 g, 61%). Anal. Calcd for C$_{40}$H$_{44}$Cu$_2$N$_{10}$O$_{22}$Tb$_2$: C, 32.9; H, 3.0; N, 9.6. Found: C, 32.7; H, 2.9; N, 9.5. Characteristic IR absorptions (KBr): 1641, 1620, 1600, 1584, 1540, 1448, 1252 cm^{-1}.

[L^{4}CuTb(NO$_3$)$_2$]$_2$(CH$_3$OH)$_2$ (13). This complex was obtained using [L^{4}CuK(CH$_3$OH)](CH$_3$OH)$_{0.5}$ (0.10 g, 1.9 × 10^{-4} mol) and Tb(NO$_3$)$_3$·6H$_2$O (0.10 g, 2.2 × 10^{-4} mol). Crystals were obtained by slow diffusion of methanol solutions of the two starting materials. Yield: (0.07 g, 54%). Anal. Calcd for C$_{42}$H$_{50}$Cu$_2$N$_8$O$_{24}$Tb$_2$: C, 33.7; H, 3.4; N, 7.5. Found: C, 33.3; H, 3.2; N, 7.3. Characteristic IR absorptions (KBr): 1634, 1580, 1545, 1465, 1264 cm^{-1}

[L^{8}CuGd(NO$_3$)$_2$(H$_2$O)]$_2$ (14). This complex was obtained using [L^{8}CuK(CH$_3$OH)] (0.28 g, 5.4 × 10^{-4} mol) and Gd(NO$_3$)$_3$·6H$_2$O (0.26 g, 5.8 × 10^{-4} mol). Yield: (0.28 g, 70%). Anal. Calcd for C$_{42}$H$_{50}$Cu$_2$Gd$_2$N$_8$O$_{24}$: C, 33.8; H, 3.4; N, 7.5. Found: C, 33.3; H, 3.2; N, 7.2. Characteristic IR absorptions (KBr): 1634, 1581, 1547, 1519, 1473, 1228 cm^{-1}.

[L^{9}CuGd(NO$_3$)$_2$(H$_2$O)]$_2$ (15). This complex was obtained using [L^{9}CuK](C$_3$H$_6$O) (0.25 g, 5 × 10^{-4} mol) and Gd(NO$_3$)$_3$·6H$_2$O (0.24 g, 5.3 × 10^{-4} mol). Yield: (0.30 g, 80%). Anal. Calcd for C$_{38}$H$_{42}$Cu$_2$Gd$_2$N$_8$O$_{22}$: C, 32.5; H, 3.0; N, 8.0. Found: C, 32.1; H, 3.2; N, 7.7. Characteristic IR absorptions (KBr): 1642, 1605, 1579, 1546, 1456, 1223 cm^{-1}.

[L^{9}CuGd(C$_7$H$_6$NO$_2$)$_2$]$_2$ (16). A methanol solution of salicylamide (0.15 g, 1.1 × 10−3 mol) and triethylamine (0.12 g, 1.1 × 10−3 mol) was added to [L^{9}CuK](C$_3$H$_6$O) (0.25 g, 5 × 10^{-4} mol) dissolved in methanol (15 mL). Then the addition of Gd(NO$_3$)$_3$·6H$_2$O (0.24 g, 5.3 × 10^{-4} mol) with stirring yielded a precipitate that was filtered off, washed with methanol and diethyl ether, and dried. Yield: (0.30 g, 80%). Anal. Calcd for C$_{66}$H$_{62}$Cu$_2$Gd$_2$N$_8$O$_{16}$: C, 47.6; H, 3.7; N, 6.7. Found: C, 47.2; H, 3.4; N, 6.4. Characteristic IR absorptions (KBr): 1639, 1602, 1570, 1538, 1242 cm^{-1}.

X-ray Crystallography. The X-ray data for compounds **5**, **12**, and **13** were collected on a Stoe Imaging Plate Diffractometer System (IPDS) equipped with an Oxford Cryosystems cooler device using a graphite monochromator (λ = 0.71073 Å). Data were collected[16] using φ oscillation (**5**) or rotation (**12**, **13**) movement with the crystal-to-detector distance equal to 70, 70, and 80 mm for **5**, **12**, and **13**, respectively (φ = 0.0−249.6°, $\Delta\varphi$ = 1.6° for **5**, φ = 0.0−200°, $\Delta\varphi$ = 2.0° for **12,** and φ = 0.0−200°, $\Delta\varphi$ = 1.5° for **13**).

(16) *STOE, IPDS Manual*, version 2.93; Stoe & Cie: Darmstadt, Germany, 1997.

Table 1. Crystallographic Data for Complexes **1**, **5**, **12**, and **13**

	1	**5**	**12**	**13**
formula	$C_{21.5}H_{27}CuKN_2O_{6.5}$	$C_{33}H_{41}N_7NiO_{11}$	$C_{20}H_{22}CuN_5O_{11}Tb$	$C_{21}H_{25}CuN_4O_{12}Tb$
fw	520.09	770.44	730.89	747.91
space group	*C*2/*c*	$P2_1/n$ (No. 14)	$P\bar{1}$	*C*2/*c*
a (Å)	27.528(2)	11.0760(9)	8.6821(17)	25.475(5)
b (Å)	7.0944(7)	21.4542(17)	11.848(2)	12.934(3)
c (Å)	22.9140(18)	15.3362(14)	11.928(2)	15.023(3)
α (deg)			81.77(3)	
β (deg)	92.130(6)	101.474(1)	89.17(3)	91.06(3)
γ (deg)			85.49(3)	
V ($Å^{-3}$)	4471.9(7)	3571.5(5)	1210.6(4)	4949.0(17)
Z	8	4	2	8
ρ_{calcd} (g cm^{-3})	1.545	1.433	2.005	2.008
λ (Å)	0.71073	0.71073	0.71073	0.71073
T (K)	180	293	240	180
μ(Mo Kα) (mm^{-1})	1.207	0.613	3.846	3.767
R_1[a] obsd, all	0.0363, 0.0491	0.0413, 0.0669	0.0210, 0.0285	0.0682, 0.0771
R_2[b] obsd, all	0.0789, 0.0831	0.0907, 0.1042	0.0469, 0.0484	0.1789, 0.1823

[a] $R = \sum||F_o| - |F_c||/\sum|F_o|$. [b] $R_w = [\sum w(|F_o^2| - |F_c^2|)^2/\sum w|F_o^2|^2]^{1/2}$.

Crystallographic measurements for **1** were carried out with the Oxford-Diffraction XCALIBUR CCD diffractometer using graphite-monochromated Mo Kα radiation. The crystals were placed 60 mm from the CCD detector. More than a hemisphere of reciprocal space was covered by the combination of four sets of exposures; each set had a different *φ* angle (0, 90, 180, 270°). Coverage of the unique set is 99.8% complete up to $2\theta = 52°$. The unit cell determination and data integration were carried out using the CrysAlis package of Oxford Diffraction.[17] Intensity data were corrected for the Lorentz and polarization effects. All the structures were solved by direct methods using SHELXS-97[18] and refined by full-matrix least-squares on F_o^2 with SHELXL-97[19] with anisotropic displacement parameters for non-hydrogen atoms. All H atoms attached to carbon were introduced in the calculations in idealized positions using the riding model. To better fit the electron density in compound **13**, a model in which the solvate methanol molecule is disordered into two resolvable orientations, with common positions for the carbon atom, was applied. Scattering factors were taken from ref 20. The molecular plot was obtained using the ZORTEP program.[21] Crystal data collection and refinement parameters are given in Table 1, while selected bond distances and angles are gathered in Table 2.

Physical Measurements. Elemental analyses were carried out at the Laboratoire de Chimie de Coordination Microanalytical Laboratory in Toulouse, France, for C, H, and N. IR spectra were recorded on a GX system 2000 Perkin-Elmer spectrophotometer. Samples were run as KBr pellets. Magnetic data were obtained with a Quantum Design MPMS SQUID susceptometer. All samples were 3 mm diameter pellets molded from ground crystalline samples. Magnetic susceptibility measurements were performed in the 2−300 K temperature range in a 0.1 T applied magnetic field, and diamagnetic corrections were applied using Pascal's constants.[22] Isothermal magnetization measurements were performed up to 5 T at 2 K. The magnetic susceptibilities have been computed by exact calculations of the energy levels associated with the spin Hamiltonian through diagonalization of the full matrix with a general program for axial symmetry[23] and with the MAGPACK program package[24] in the case of magnetization. Least-squares fittings were accomplished with an adapted version of the function-minimization program MINUIT.[25] The ac measurements were carried out in a

Table 2. Selected Bond Lengths (Å) and Angles (deg) for Complexes **1**, **5**, **12**, and **13**

	$[L^7Ni](C_5H_{12}N)_2(C_6H_2N_3O_7)$ (**5**)		
Ni−O(1)	1.8611(17)	Ni−N(1)	1.842(2)
Ni−O(2)	1.8400(17)	Ni−N(2)	1.851(2)
O(1)−Ni−O(2)	83.97(8)	O(2)−Ni−N(1)	175.76(9)
O(1)−Ni−N(1)	94.31(9)	O(2)−Ni−N(2)	95.39(9)
O(1)−Ni−N(2)	174.81(10)	N(1)−Ni−N(2)	86.66(10)
	$[L^4CuK(CH_3OH)](CH_3OH)_{0.5}$ (**1**)		
Cu(1)−O(1)	1.896(2)	Cu(1)−N(1)	1.915(2)
Cu(1)−O(2)	1.919(2)	Cu(1)−N(2)	1.949(2)
K(1)−O(1)	2.650(2)	K(1)−O(3)	2.701(2)
K(1)−O(2)	2.665(2)	K(1)−O(4)	2.775(2)
K(1)−O(6)	2.758(2)		
O(1)−Cu(1)−O(2)	88.36(7)	O(2)−Cu(1)−N(1)	177.36(8)
O(1)−Cu(1)−N(1)	93.98(8)	O(2)−Cu(1)−N(2)	92.28(8)
O(1)−Cu(1)−N(2)	177.01(8)	N(1)−Cu(1)−N(2)	85.44(8)
	$[L^4CuTb(NO_3)_2(DMF)]_2$ (**12**)		
Cu(1)−O(1)	1.888(2)	Cu(1)−N(1)	1.928(3)
Cu(1)−O(2)	1.941(2)	Cu(1)−N(2)	1.905(3)
Tb(1)−O(1)	2.319(2)	Tb(1)−O(3)′	2.293(2)
Tb(1)−O(2)	2.462(2)	Tb(1)−O(5)	2.330(2)
Tb(1)−O(4)	2.628(2)	Tb(1)−O(6)	2.492(2)
Tb(1)−O(8)	2.529(2)	Tb(1)−O(10)	2.491(3)
Tb(1)−O(11)	2.448(3)		
O(1)−Cu(1)−O(2)	85.68(9)	O(1)−Cu(1)−N(1)	94.23(10)
O(2)−Cu(1)−N(2)	95.27(11)	N(1)−Cu(1)−N(2)	85.70(11)
Cu(1)−O(1)−Tb(1)	107.45(9)	Cu(1)−O(2)−Tb(1)	100.46(9)
	$[L^7CuTb(NO_3)_2]_2(CH_3OH)_2$ (**13**)		
Cu(1)−O(1)	1.891(10)	Cu(1)−N(1)	1.904(12)
Cu(1)−O(2)	1.928(10)	Cu(1)−N(2)	1.910(12)
Tb(1)−O(1)	2.344(10)	Tb(1)−O(3)′	2.285(10)
Tb(1)−O(2)	2.339(9)	Tb(1)−O(4)	2.611(10)
Tb(1)−O(5)	2.572(10)	Tb(1)−O(6)	2.471(10)
Tb(1)−O(7)	2.463(11)	Tb(1)−O(9)	2.465(10)
Tb(1)−O(10)	2.472(10)		
N(1)−Cu(1)−N(2)	86.7(5)	O(1)−Cu(1)−N(1)	95.7(5)
O(2)−Cu(1)−O(1)	81.9(4)	O(2)−Cu(1)−N(2)	95.8(5)
Cu(1)−O(1)−Tb(1)	107.1(4)	Cu(1)−O(2)−Tb(1)	106.0(4)

(17) *CrysAlis RED*, version 1.170.32; Oxford Diffraction Ltd.: Abingdon, U.K., 2003.
(18) Sheldrick, G. M. *SHELXS-97. Program for Crystal Structure Solution*; University of Göttingen: Göttingen, Germany, 1990.
(19) Sheldrick, G. M. *SHELXL-97. Program for the Refinement of Crystal Structures from Diffraction Data*; University of Göttingen: Göttingen, Germany, 1997.
(20) *International Tables for Crystallography*; Kluwer Academic Publishers: Dordrecht, The Netherlands, 1992; Vol. C.
(21) Zsolnai, L.; Pritzkow, H.; Huttner, G. *ZORTEP. Ortep for PC, Program for Molecular Graphics*; University of Heidelberg: Heidelberg, Germany, 1996.
(22) Pascal, P. *Ann. Chim. Phys.* **1910**, *19*, 5.

Scheme 1

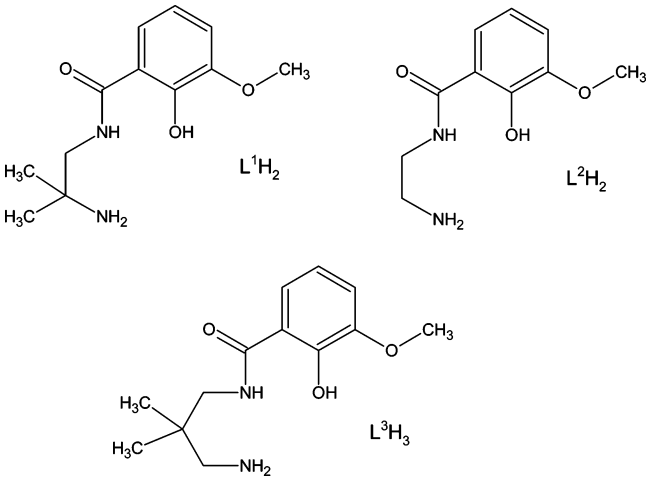

3.0 G ac field oscillating at different frequencies (from 50 to 1000 Hz) and with a zero dc field.

Results and Discussion

Syntheses. The compartmental ligands L^4H_3, L^5H_3, L^6H_3, L^7H_3, L^8H_3, and L^9H_3 used in this study are disymmetric and trianionic for they possess one amide and two phenol functions. They have been prepared according to an experimental stepwise procedure described previously.[13,26] In the present case, the ester, which is not commercial, has been prepared by reaction of 3-methoxysalicylic acid with dicyclohexylcarbodiimide in the presence of phenol in excess and THF as solvent. Reaction of the phenyl 3-methoxysalicylate with the desired diamine, 1,2-diamino-2-methylpropane or 1,3-diamino-2,2-dimethylpropane in 2-propanol or dichloromethane, yields the amide function of the ligand. Because of the mild experimental conditions pure half-unit ligands L^1H_2 and L^3H_2, in which only one function of the diamine reactant has been involved in the reaction process, are isolated in good yields (Scheme 1). When similar reaction conditions are used with 1,2-diaminoethane, a mixture of the half-unit and of the symmetrical ligand is obtained, but these two ligands can be easily separated. Further reaction of the L^1H_2, L^2H_2, and L^3H_2 half-unit ligands with orthovanillin, 3-ethoxysalicylaldehyde, or salicylaldehyde yields L^4H_3, L^5H_3, L^6H_3, L^7H_3, L^8H_3, and L^9H_3 (Scheme 2). These ligands include an inner N_2O_2 coordination site with one amide, one imine, and two phenol functions and an outer O_2O_2 or O_2O coordination site involving again the two phenol functions and one or two oxygen atoms of the methoxy groups. The monometallic complexes are readily obtained by reaction of the ligand prepared in situ in a methanol solution with copper(II) or nickel acetate in the presence of potassium hydroxide or piperidine as deprotonating agents. The desired complexes are obtained as crystals from the resulting reaction media or powders with satisfying yields. The heterometallic Cu−Ln complexes (Ln = Gd, Tb) were isolated by reaction of these precursors with nitrate or chloride lanthanide salts in methanol. According to chemical analysis, they are well represented by $L^nCuGd(X)_2$, with or without water or methanol molecules (X = nitrato or salicylamidato anion). As a consequence of the trianionic nature of the related ligands, the electroneutrality of the dimetallic complexes necessitates the presence of only two nitrato anions. The decrease in the number of nitrato anions (from three with a dianionic ligand to two for a trianionic one) releases two coordination sites onto the gadolinium center and possibly favors the coordination of the 4f ion to the oxygen atom of the amido group of a neighboring dinuclear entity. Nitrato ions can be easily replaced by a ligand such as salicylamide under its deprotonated form.

Scheme 2

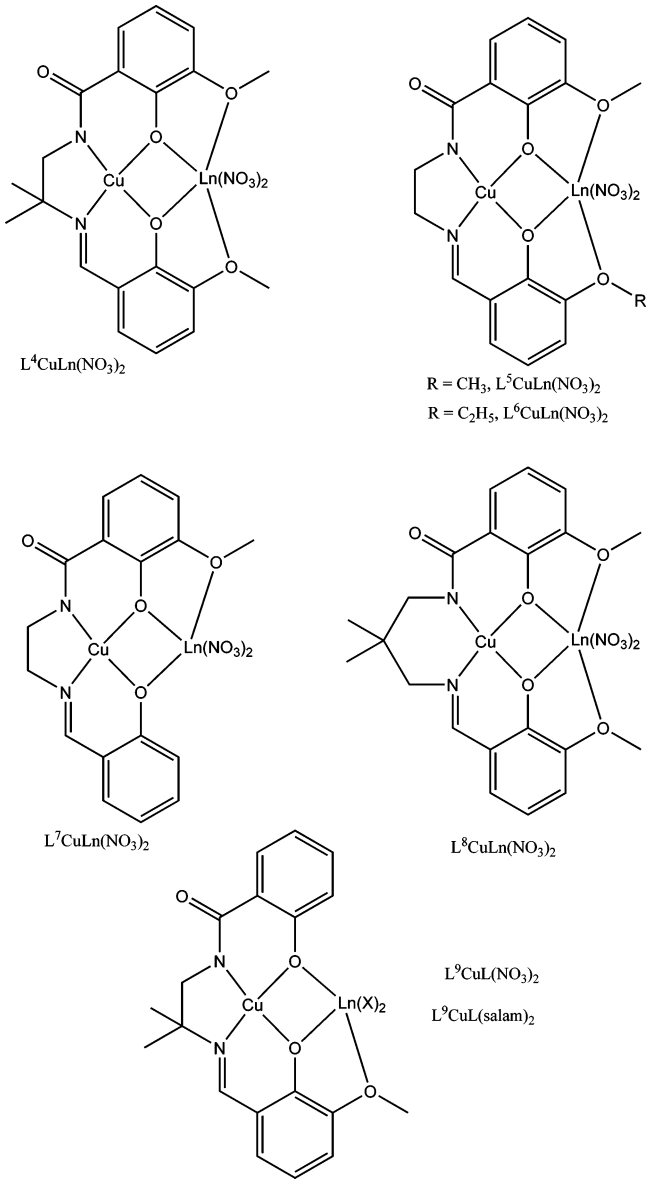

(23) Clemente-Juan, J. M.; Mackiewicz, C.; Verelst, M.; Dahan, F.; Bousseksou, A.; Sanakis, Y.; Tuchagues, J.-P. *Inorg. Chem.* **2002**, *41*, 1478.
(24) (a) Borrás-Almenar, J. J.; Clemente-Juan, J. M.; Coronado, E.; Tsukerblat, B. S. *Inorg. Chem.* **1999**, *38*, 6081. (b) Borrás-Almenar, J. J.; Clemente-Juan, J. M.; Coronado, E.; Tsukerblat, B. S. *J. Comput. Chem.* **2001**, *22*, 985.
(25) James, F.; Roos, M. MINUIT Program, A System for Function Minimization and Analysis of the Parameters Errors and Correlations. *Comput. Phys. Commun.* **1975**, *10*, 345.
(26) Daidone, G.; Raffa, D.; Maggio, B.; Plescia, S.; Matera, M.; Caruso, A. *Farmaco, Ed. Sci.* **1990**, *45*, 285.

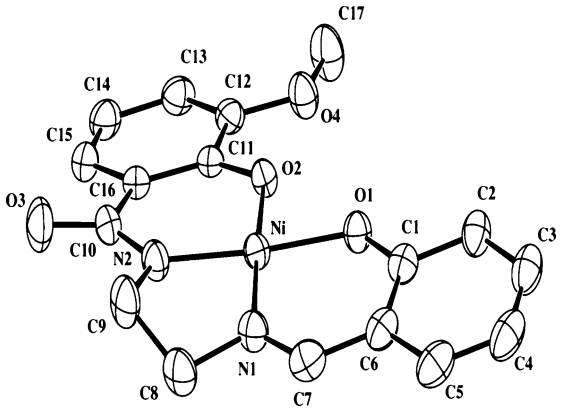

Figure 1. Zortep plot of the anionic L^7Ni entity for **5** with ellipsoids drawn at the 50% probability level and the atomic labeling scheme.

Description of the Structures. The asymmetric unit of complex **5** is composed of the L^7Ni monoanionic entity with its cationic piperidinium counterpart and of a piperidinium picrate. As expected, the nickel^{II} ion is in the inner trianionic N_2O_2 coordination site, connected in a square planar environment to the amido and imine nitrogen and the two phenoxo oxygen atoms, with similar Ni−O (1.840(2), 1.861(2) Å) and Ni−N (1.842(2), 1.851(2) Å) bond lengths, while the amide oxygen atom O(3) is not involved in coordination (Figure 1). The central Ni−N−C−C−N five-membered ring of the diamino chain is gauche with a δ conformation. One piperidinium ion makes two N(6)−H···O hydrogen bonds with the O(1) phenoxo atom of L^7Ni (N(6)···O(1) = 2.846(3) Å, N(6)−H = 0.90 Å, N(6)−H···O(1) = 1.99 Å, ∠NHO = 157.3°) and the O(5) phenoxo atom of picrate (N(6)···O(5) = 2.739(3) Å, N(6)−H = 0.90 Å, N(6)−H···O(5) = 1.97 Å, ∠NHO = 142.2°) inside the asymmetric unit, while the other one links two L^7Ni entities through two hydrogen bonds involving the other phenoxo O(2) atom (N(7)···O(2) = 2.888(3) Å, N(6)−H = 0.90 Å, N(6)−H···O(1) = 1.99 Å, ∠NHO = 172.0°) and the amide oxygen atom (N(7)···O(3′) = 2.675(3) Å, N(6)−H = 0.90 Å, N(6)−H···O(1) = 1.78 Å, ∠NHO = 174.9°) of a neighboring entity, so that all the oxygen atoms of the L^7Ni units are engaged in hydrogen bonds (Figure S1). As a result, these numerous short intermolecular contacts bind all the components of the structure and give a 3D network, which must be responsible for the presence of the picrate ion in the final L^7Ni complex.

Crystal **1** belongs to the monoclinic system and crystallizes in the *C*2/*c* space group, with neutral [L^4CuK(MeOH)] species as crystallographically asymmetric entities. In the crystal lattice these dinuclear complexes are associated into chains by H-bonds involving coordinated methanol molecules and the amide oxygen of the neighboring molecules (O(6)−H = 0.86(1), O(6)···O(5)′ (x, $-y$, $0.5 + z$) = 2.672(3), O(6)H···O(5)′ = 1.82(1) (Å), ∠OHO = 171(4)°) (Figure 2). The additional solvate methanol molecules are not coordinated but are hydrogen bonded to the amide oxygen atoms (O(7)−H = 0.89(5), O(7)···O(5) = 2.823(5), O(7)H···O(5) = 1.94(5) Å, ∠OHO = 171(4)°) (Figure S2). The copper(II) ion is in the trianionic N_2O_2 inner coordination site with

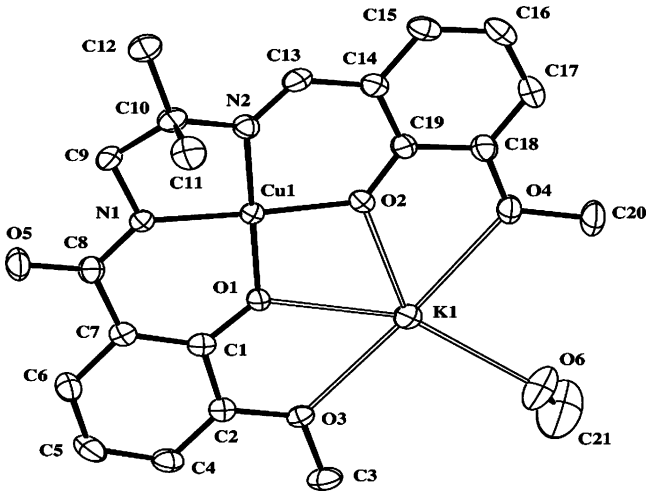

Figure 2. Fragment of the infinite hydrogen-bonded chain in the crystal structure of [L^4CuK(CH_3OH)](CH_3OH)$_{0.5}$ (**1**), including the atom labeling scheme. The thermal ellipsoids are drawn at the 40% probability level.

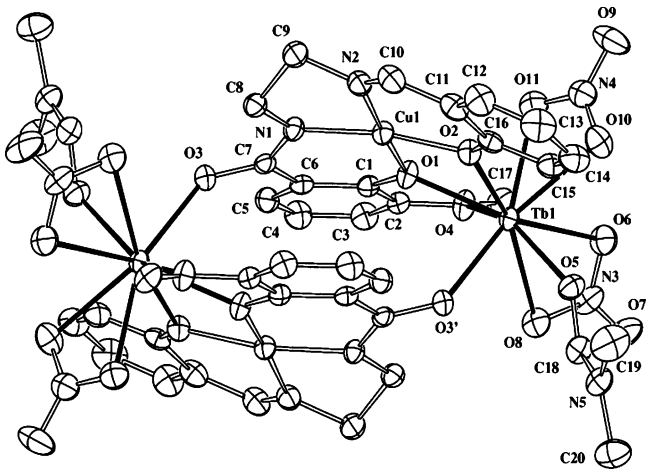

Figure 3. View of the tetranuclear entity [L^7CuTb(NO_3)$_2$(DMF)]$_2$ (**12**). The thermal ellipsoids are drawn at the 40% probability level.

a square planar environment. The Cu−O (1.915(2)−1.949(2) Å) and Cu−N (1.896(2)−1.919(2) Å) bonds are slightly longer than the Ni−O and Ni−N bonds of **5**. The potassium ion is pentacoordinated to the four oxygen atoms of the outer O_2O_2 site and to a methanol molecule. As reported earlier, the K−O bond lengths[27] depend on the nature of the oxygen atom, the shortest bond distances corresponding to the phenoxo oxygens (2.650(2)−2.665(2) Å) and the longest ones to the methoxy groups (2.701(2)−2.775(2) Å) and methanol (2.757(3) Å).

The main structural particularity of **12** and **13** is that two heteronuclear Cu−Tb entities are assembled through the oxygen atoms of the amido groups to form a double (Cu−N−C−O−Tb) bridge which leads to tetranuclear entities regardless of the nature of the outer coordination site, O_2O_2 or O_2O, as represented in Figures 3 and 4. As expected, the copper ions adopt a square planar coordination in the inner N_2O_2 site, while the terbium ions are in the outer (O_2O_2 or O_2O) sites. The two ions are doubly bridged one to the other

(27) Miyasaka, H.; Matsumoto, N.; Okawa, H.; Re, N.; Gallo, E.; Floriani, C. *J. Am. Chem. Soc.* **1996**, *118*, 981.

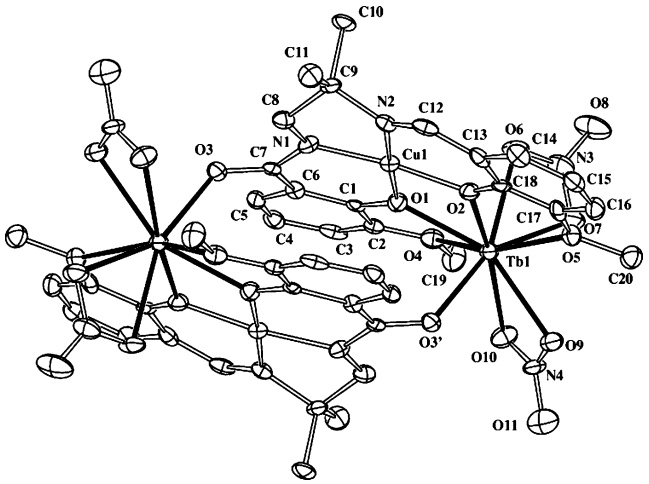

Figure 4. Molecular structure of $[L^4CuTb(NO_3)_2]_2(CH_3OH)_2$ (**13**). The thermal ellipsoids are drawn at the 40% probability level.

by two phenoxo oxygen atoms belonging to the L^7 or L^4 ligands with Cu···Tb separations of 3.417(2) and 3.4006(8) Å, respectively. These bridging networks, Cu−$(O)_2$−Tb, are not far from being planar since the dihedral angles between the (OCuO) and (OTbO) planes are equal to 6.9(2)° and 6.3(3)° for **12** and **13**, respectively. The terbium ions are nine coordinate. In addition to the two bridging phenoxo oxygen atoms, they complete their environments with four oxygen atoms coming from two bidentate η^2-coordinated nitrato ions, the amide oxygen not involved in the coordination site, and one or two oxygen atoms from the OMe sidearms. In the case of the L^7 ligand, the missing oxygen atom is replaced by an oxygen atom of a dimethylformamide molecule. The Tb−O bond lengths depend on the nature of the oxygen atoms; they vary from 2.319(2) to 2.628(2) Å for **12** and from 2.285(10) to 2.611(10) Å for **13**. The bonds issued from the amido oxygen (2.293(2) Å for **12** and 2.285(10) Å for 13) are shorter than those from the phenoxo oxygens, the longest ones being related to the methoxy sidearms and the nitrato ions. These bonds are comparable in the two complexes, except for the $Tb-O_{phenoxo}$ bond coming from the phenyl ring devoid of the methoxy group in **12** which is longer (Tb(1)−O(2) = 2.462(2) Å), while the $Tb-O_{DMF}$ bond(Tb(1)−O(5) = 2.330(2) Å) is in the range of the other $Tb-O_{phenoxo}$ bond lengths.

In the tetranuclear complexes **12** and **13**, the shortest metal−metal separations that concern Cu(II) ions not related by a material link are equal to 5.232(1) and 5.001(3) Å, respectively. The separations between the Cu(II) and Gd(III) ions bound to each other through the amido oxygen are equal to 5.730(2) and 5.535(2) Å, respectively. The intermolecular metal−metal separations which are larger than 6.8 Å for **12** and 7.2 Å for **13** preclude any significant interaction of magnetic nature between these tetranuclear units.

Magnetic Properties. The magnetic susceptibility of the Cu−Gd (**8**, **10**, **11**, **14**, **15**, **16**) and Cu−Tb (**9**, **12**, **13**) complexes have been measured in the 2−300 K temperature range in a 0.1 T applied magnetic field. The magnetic behavior of the Cu−Gd complexes will be examined first. As an example, the thermal variation of the $\chi_M T$ versus T plot of complex **8** is shown in Figure 5. χ_M is the molar magnetic susceptibility of the tetranuclear complex, corrected for the diamagnetism of the ligands.[22] At 300 K, $\chi_M T$ is equal to 16.65 cm^3 K mol^{-1}, which is attributable to four (two Cu(II) and two Gd(III)) uncoupled ions. Lowering the temperature causes χ_MT to increase and reach a value of 30.56 cm^3 K mol^{-1} at 2 K, which is larger than expected (2 × 10 cm^3 K mol^{-1}) for two uncorrelated pairs of ferromagnetically coupled Cu(II) and Gd(III) ions but smaller than the value attributable (36 cm^3 K mol^{-1}) to a $S = 8$ spin state resulting from the ferromagnetic coupling of two (Cu, Gd) pairs. Such behavior is consistent with the simultaneous occurrence of two ferromagnetic (Cu, Gd) interactions which would operate within each (Cu, Gd) pair (J) and between two pairs (j), respectively. A quantitative analysis based on a "dimer-of-dimer" model directly derived from the structural data and using the Hamiltonian $H = -J(S_{Cu}S_{Gd} + S_{Cu'}S_{Gd'}) - j(S_{Cu}S_{Gd'} + S_{Cu'}S_{Gd})$ leads to $J = 7.96$ cm^{-1}, $j = 0.82$ cm^{-1}, and $g = 1.995$. The agreement factor R ($R = \sum[(\chi T)_{obsd} - (\chi T)_{calcd}]^2/\sum[(\chi T)_{obsd}]^2$) is excellent ($R = 1 \times 10^{-5}$). The importance of the two coupling constants characterizing complex **8** differ by an order of magnitude so that their respective pathways are easily recognized. The J value of 7.96 cm^{-1} is quite reminiscent of those reported[28] for structurally characterized heterodinuclear complexes with a bridging (CuO_2Gd) network. The second interaction, $j = 0.82$ cm^{-1}, may be related to the amido bridge (Cu−N−C−O−Gd′).[15]

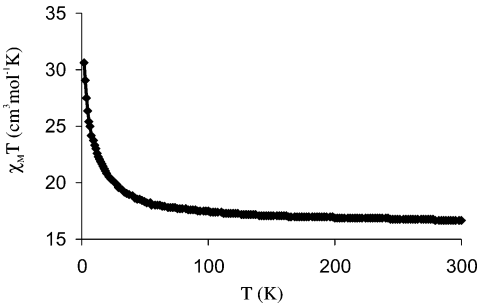

Figure 5. Thermal dependence of $\chi_M T$ for **8** at 0.1 T. The full line corresponds to the best data fit.

Confirmation of the nature of the ground state and, consequently, of the nuclearity of complex **8** is given by the field dependence of the magnetization, M, at 2 K. The experimental values of M fit correctly the Brillouin function for a $S = 8$ spin state. (Figure 6). Furthermore, increasing the field up to 5 T causes the magnetization to approach the saturation value of 16 Nβ units consistent with a $S = 8$, $g = 2$ system.

The magnetic studies of the other Cu−Gd complexes give the results reported in Table 3, with the thermal variations of the $\chi_M T$ versus T plots reported in Supporting Information (Figures S3−S7). To check if a nuclearity change was possible, we introduced some ligands modifications to the length of the diamino chains with two or three carbon atoms, the presence or absence of two methyl groups on the two

(28) (a) Costes, J. P.; Dahan, F.; Dupuis, A.; Laurent, J. P. *Inorg. Chem.* **1997**, *36*, 3429. (b) Novitchi, G.; Costes, J. P.; Donnadieu, B. *Eur. J. Inorg. Chem.* **2004**, 1808.

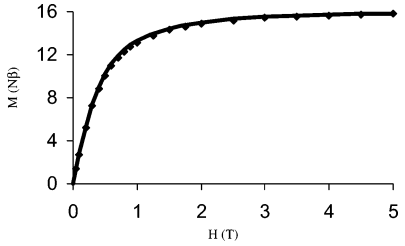

Figure 6. Field dependence of the magnetization for **8** at 2 K. The solid line corresponds to the $S = 8$ ground state.

Table 3. Results of the Magnetic Studies of Cu−Gd Complexes

complex	J (cm^{-1})	j (cm^{-1})	g	R
$[L^4CuGd(NO_3)_2]_2$ [a]	6.94	0.58	1.99_6	1×10^{-5}
$[L^5CuGd(NO_3)_2]_2$ (**8**)	7.96	0.82	1.99_5	1×10^{-5}
$[L^6CuGd(NO_3)_2]_2$ (**10**)	3.94	0.61	2.01	1×10^{-4}
$[L^7CuGd(NO_3)_2(H_2O)]_2$ (**11**)	2.80	0.64	1.98_5	1×10^{-4}
$[L^8CuGd(NO_3)_2(H_2O)]_2$ (**14**)	4.16	0.34	1.99_8	6×10^{-5}
$[L^9CuGd(NO_3)_2(H_2O)]_2$ (**15**)	5.89	0.82	1.99_6	4×10^{-5}
$[L^9CuGd(C_7H_6NO_2)_2]_2$ (**16**)	2.56	0.07	1.99	1×10^{-4}

[a] Ref 15.

carbon atom diamino chain, or the nature of the outer coordination for the Ln ion, O_2O_2 or O_2O. We also replaced the nitrato anions chelated to the Ln ion with deprotonated salicylamido ligands. The changes made the entire set of complexes behave as tetranuclear entities with two ferromagnetic interactions. A look at the results shows that the j value is in the 0.6−0.8 cm^{-1} interval, except for two cases. In the first case, substitution of nitrato anions (complex **15**) by the more voluminous salicylamido ligands in $[L^9CuGd(C_7H_6NO_2)_2]_2$ (**16**) must lengthen the $Gd-O_{amide}$ bond so that a decrease of the interaction parameter through the amide function is observed. An intermediate j value is found in $[L^8CuGd(NO_3)_2(H_2O)]_2$ (**14**). The L^8 ligand with three carbon atoms in the diamino chain must induce a greater deformation of the $(Cu-Gd)_2$ core. We have previously proposed[29] the existence of a relationship between the magnitude of the ferromagnetic interaction J and the dihedral angle α between the two halves, (OCuO) and (OGdO), of the double bridge. Indeed, the best J value is obtained with the $[L^5CuGd(NO_3)_2]_2$ (**8**) complex, which implies that the α value in **8** is lower than 6.0°.[15] As a consequence, the planarity of the heterodinuclear L^5CuGd unit along with the removal of the methyl groups of the L^4 diamino chain allow a better approach of the two dinuclear units and, consequently, a better j value. Some discrepancies in the J values are surprising. $[L^5CuGd(NO_3)_2]_2$ (**8**) and $[L^6CuGd(NO_3)_2]_2$ (**10**) have the same bridging cores and only differ by the replacement of a methoxy group by an ethoxy one. Nevertheless we observe a decrease of the J parameter from 7.96 to 3.94 cm^{-1}, along with a decrease of the j value (from 0.82 to 0.61 cm^{-1}). For the tetranuclear entities with an outer O_2O site, the methoxy group can be positioned on the phenyl ring bearing the amide function (L^7 ligand) or on the phenyl ring linked to the imine function (L^9 ligand). Surprisingly, the J value varies from 2.80 cm^{-1} for **11** ($[L^7CuGd(NO_3)_2(H_2O)]_2$) to 5.89 cm^{-1} for **15** ($[L^9CuGd(NO_3)_2(H_2O)]_2$). The presence of the methoxy substituent and the amide function on the same phenyl ring (L^7) must be responsible for a greater deformation of the $Cu-O_2-Gd$ core in comparison to the case where the amide function is brought by one phenyl ring and the methoxy group by the other one (L^9). An example of a ligand closely related to L^9 (the difference comes from the absence of the two methyl substituents on the diamino chain) has been previously reported in the literature.[14] It is not surprising to see that the resulting tetranuclear complex $[LCuGd(hfa)_2]_2$ gives an intramolecular interaction of 6.2 cm^{-1}, similar to the value (5.89 cm^{-1}) found in **15** ($[L^9CuGd(NO_3)_2(H2O)]_2$). The interactions through the amide function are markedly different, 2.4 cm^{-1} instead of 0.82 cm^{-1}. Such a difference cannot be explained by either the presence of methyl groups in the diamino chain or the $Gd-O_{amide}$ bond lengths (from 2.275(3) to 2.293(2) Å) which are always the shortest ones within the gadolinium coordination sphere. It seems that changes in the gadolinium coordination spheres from nine-coordinate in our compounds to eight-coordinate in the Matsumoto's complex[14] are responsible for these different j parameters. Replacement of the chelating nitrato ions by hfa ligands with different bite sizes modify the geometrical environment of the Gd ion. Furthermore, they allow a better insulation of the tetranuclear units.

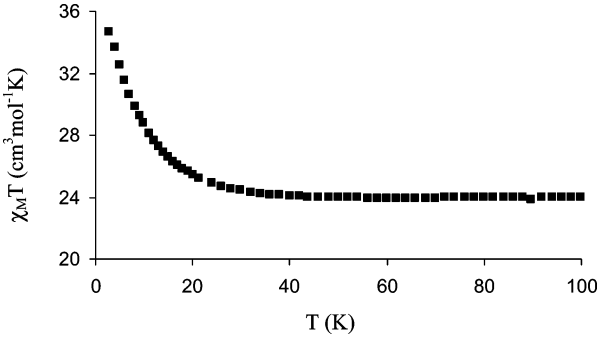

Figure 7. Thermal dependence of $\chi_M T$ for **13** at 0.1 T.

The $\chi_M T$ versus T curve for the $[Cu-Tb]_2$ complex **13** is shown in Figure 7. From 300 to 44 K, $\chi_M T$ decreases slightly from 24.1 to 24.0 $cm^3\ mol^{-1}$ K and then increases to 33.2 $cm^3 mol^{-1}$ K at 2 K. The last value is large compared to the value expected for four insulated ions. On the basis of the free ion value (11.75 $cm^3\ mol^{-1}$ K) for each Tb^{3+} ($^7F_6$) and a contribution of 0.37 $cm^3\ mol^{-1}$ K for each copper ion, the calculated value is c.a. 24.2 $cm^3\ mol^{-1}$ K. Interestingly, this is practically the experimental value observed at 300 K. We know that the Tb^{3+} ion possesses a large orbital momentum with strong spin−orbit coupling which is responsible for the decrease of the $\chi_M T$ product as T decreases. But if we remember that the Cu−Tb interaction has been reported to be ferromagnetic in few examples,[30,31] this magnetic behavior (Figure 7) shows the existence of ferromagnetic interactions through the double phenoxo bridge and the single amido bridge, as in the $[Cu-Gd]_2$ complexes. Furthermore, the coexistence of antagonist effects in the $[Cu-Tb]_2$ species

(29) Costes, J. P.; Dahan, F.; Dupuis, A.; Laurent, J. P. *Inorg. Chem.* **2000**, *39*, 169.

(30) Kahn, M. L.; Mathonière, C.; Kahn, O. *Inorg. Chem.* **1999**, *39*, 3692.

(31) Costes, J. P.; Dahan, F.; Dupuis, A.; Laurent, J. P. *Chem.—Eur. J.* **1998**, 4, 1616.

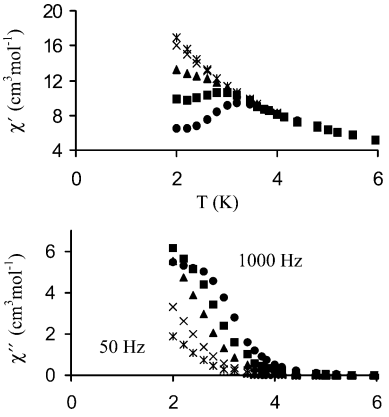

Figure 8. Frequency dependence of the in-phase and out-of-phase susceptibilities against temperature in a 3 G AC magnetic field oscillating at different frequencies (from 50 to 1000 Hz) for complex **13**.

can easily explain the presence of a minimum in the $\chi_M T$ versus T curve.

The field dependence of the magnetization (M) has been determined. When the the applied field increases, M increases up to 10.8 Nβ at 5 T but does not reach the expected saturation value (9 Nβ for each Tb^{3+} and 1 Nβ for each Cu^{2+} ion). However it may be noted that it is difficult and probably meaningless to search at the present time for a quantitative description of the ground and excited states in terms of simple interaction parameters (like the coupling constant J for polynuclear transition complexes) and an appropriate quantum number in the case of a (3d, 4f) cluster in the presence of spin−orbit coupling.[14]

The results of alternating current susceptibility measurements are more significant. The data are represented in Figure 8 as the plots of the in-phase (χ'_M) and out-of-phase (χ''_M) susceptibilities versus T for different frequencies of the external field. The profile of these plots is characteristic for slow relaxation of the magnetization. Unfortunately, the maximum of χ''_M could not be observed with this setup working at temperatures higher than 1.8 K. We used therefore a micro-SQUID apparatus[32] to study the magnetization dynamics down to 0.04 K. The studies were performed on a powder of microcrystals which was thermalized using Apiezo grease. Figure 9 presents typical hysteresis loops of compounds **12** (top) and **13** (bottom), showing a temperature and field sweep rate dependent hysteresis (Figure S9). The hysteresis loops of compound **13** show a "double-S-like" curve, which is characteristic for small antiferromagnetic interactions between molecules. Because such an interaction makes the interpretation of hysteresis more complicated, we focused our studies on compound **12**, which does not show such interactions.

We studied the origin of the magnetic hysteresis of compound **12** via dc relaxation measurements. At a given temperature, the magnetization was first saturated in a high magnetic field. After the field was swept down to zero with a field sweep rate of 0.14 T/s, the magnetization decay was

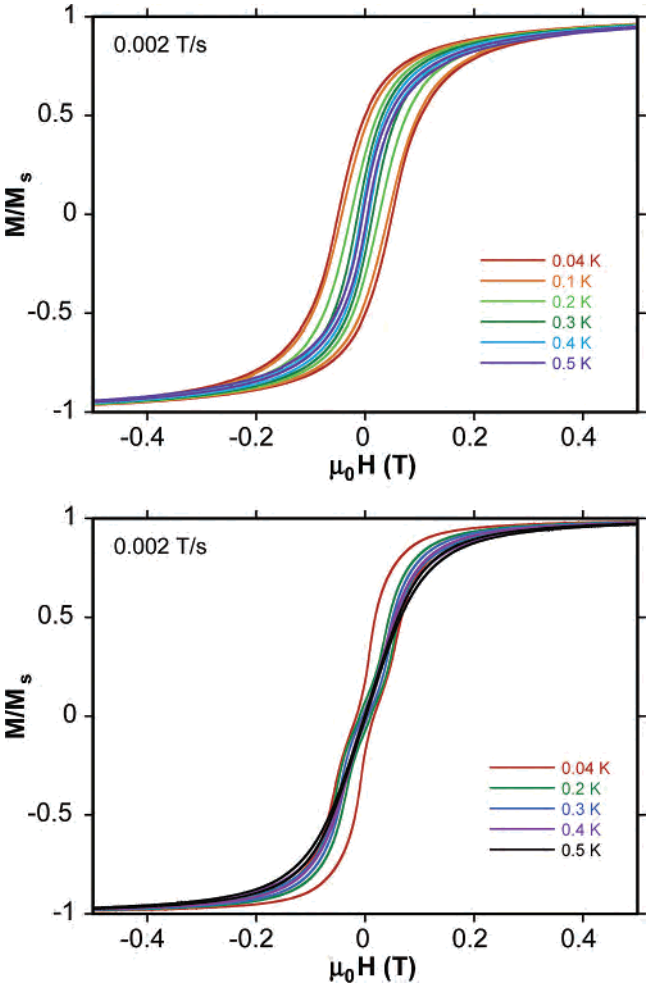

Figure 9. Hysteresis loop measurements of compounds **12** (top) and **13** (bottom) for several temperatures and a field sweep rate of 0.002 T/s. The magnetization is normalized by the saturation value, M_s, at 1.4 T.

measured as a function of time (Figure S10). Because the decay was not exponential and showed two different regimes, we used a scaling procedure of the long relaxation regime to obtain the mean relaxation time (τ). In Figure S11, the dc relaxation times are plotted into an Arrhenius plot. Two regimes are observed: (i) above 0.3 K, the thermal dependence of the relaxation time follows an Arrhenius law [$\tau = \tau_o \exp(E_a/k_B T)$ with τ_o being the preexponential factor and E_a the effective energy barrier for spin reversal] with an activation energy of $E_a/k_B = 4.2$ K and $\tau_o = 1 \times 10^{-5}$ s and (ii) below 0.3 K, the curve flattens and the relaxation rate starts to be temperature independent.

To confirm this result, we applied a method that was recently applied to SMMs[33] and SCMs[34] and that allowed a detailed understanding of the reversal mechanism. The method consists of measuring the temperature and field sweep rate dependences of the coercive fields (H_c) which is presented in Figure 10. As expected for a thermally activated process, the values of H_c increase with decreasing temperature, T, and increasing field sweep rate, $\upsilon = dH/dt$.

(32) Wernsdorfer, W.; Bonet Orozco, E.; Hasselbach, K.; Benoit, A.; Barbara, B.; Demoncy, N.; Loiseau, A.; Pascard, H.; Mailly, D. *Phys. Rev. Lett.* **1997**, 78, 1791.

(33) Wernsdorfer, W.; Murugesu, M.; Tasiopoulos, A. J.; Christou, G. *Phys. Rev. B.* **2005**, 72, 212406.

(34) Wernsdorfer, W.; Clérac, R.; Coulon, C.; Lecren, L.; Miyasaka, H. *Phys. Rev. Lett.* **2005**, 95, 237203.

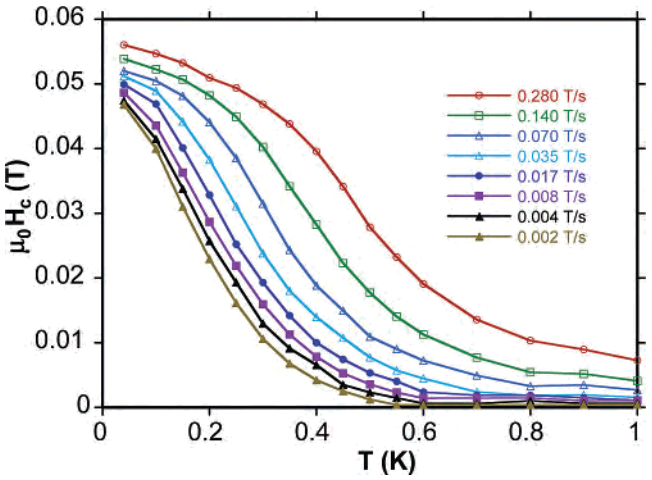

Figure 10. The coercive field, H_c, for compound **12** as a function of the temperature at several field sweep rates.

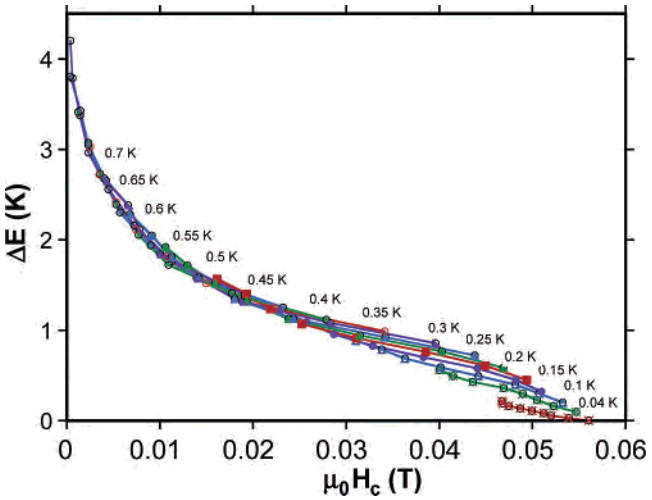

Figure 11. Field dependence of the energy barrier of compound **12** obtained from the set of H_c (T,υ) data from Figure 10.

Furthermore, all our measurements showed an almost logarithmic dependence of H_c on the field sweep rate (Figure S12). The temperature dependence of H_c flattens below ca. 0.3 K.

The field dependence of the effective energy barrier can be obtained from the set of $H_c(T,\upsilon)$ data using $\Delta E = kT \ln(c/\upsilon)$,[33,34] where the field sweeping rate is given by $\upsilon = dH/dt$, $c = H_c^0 kT/[2\tau_0 E_a(1 - H_c/H_c^0)]$, H_c^0 is the reversal field at zero temperature, E_a is the effective activation barrier at zero applied field. The result is plotted in Figure 11. One can see that ΔE is about $E_a/k_B = 4$ K at $H = 0$ which is in good agreement with the result obtained with relaxation measurements. As expected, ΔE decreases with the increasing field. Below ca. 0.3 K, the tunneling reduces the barrier to zero. The fact that no resonant tunnel transition is observed at $H = 0$ suggests that small intermolecular dipole and exchange interactions influence the tunnel process. The value of E_a/k_B (4 K) is smaller than that obtained for similar tetranuclear $[Cu-Tb]_2$ species ($E_a/k_B = 21$ K) made with a ligand closely related to L[7],[4] where the methoxy substituent is linked to the phenyl ring involved in the imine function while it is introduced in the phenyl ring bearing the amide link in L[7]. As explained below, the main difference between the Matsumoto's complex and complex **12** lies in the nature of the auxiliary ligands around Tb ions, two chelating hexafluoroacetylacetonato ligands versus two η^2-coordinated nitrato anions.

Conclusion

To sum up the present work it may be noted that the synthetic strategy based on the assembly of preformed dinuclear units has been partially successful. The addition of an amide function to the structure of a binucleating Schiff base allows the formation of a tetranuclear complex. The structural studies show that within each dinuclear (Cu−Gd) unit the two metal ions are bridged by two phenoxo oxygen atoms while the amido (N−C−O) groups link the Cu(II) and Gd′(III) ions of two neighboring dinuclear units. These structural features agree with the data of the magnetic studies which show that two types of interactions are operative. Both are ferromagnetic and result in a $S = 8$ spin ground state. The importance of the two coupling constants characterizing such complexes differ by an order of magnitude so that their respective pathways are easily recognized. The J values, varying from 2.56 to 7.96 cm^{-1}, are quite reminiscent of those (1.42−10.1 cm^{-1}) reported[28] for structurally characterized complexes with a bridging (CuO_2Gd) network. In a previous work, we have shown the role held by the dihedral angle made by the planes involving the two phenoxo bridging atoms and the 3d and 4f ions, an observation which was retained in a recent theoretical work.[35] This would explain why complexes **8** and **9**, without any CH_3 group into the diamino chain, possess dihedral angles lower than 6.0(3)°. This planarity and the absence of methyl groups on the diamino chain favor the shortening of the Gd−O(amide) bond. Indeed, the j interaction, related to the amido bridge (Cu−N−C−O−Gd′), varies from 0.34 to 0.82 cm^{-1} in the different complexes containing nitrato ions chelating the gadolinium centers, and the larger value (0.82 cm^{-1}) is associated with complex **8**. These values are far from being negligible. In the $[Cu_3Gd_2]_n$ complex,[30] each Gd(III) ion is coupled to three Cu(II) ions through oxamato groups, and the relevant constant has an estimated value of 0.15 cm^{-1}. Furthermore, when the nitrato anions are replaced by bulky ligands such as salicylamidato ligands, the j parameter decreases strongly (from 0.82 to 0.07 cm^{-1}), as a consequence of an increase of the Cu−N−C−O−Gd separation. We have also seen that changes introduced in the diamino chain (two or three carbon atoms) or in the nature of the outer coordination site (O_2O_2 or O_2O) do not modify the nuclearity of the resulting species. Despite these differences, all of the ligands used here possess only one amide function, so that the heterodinuclear species can be bridged by an unique link. A parallel arrangement of these entities should give an infinite chain $(Cu-Gd)_n$ while the head to tail arrangement observed in the structural determinations limits the nuclearity to a maximum value of four.

(35) Paulovic, J.; Cimpoesu, F.; Ferbinteanu, M.; Hirao, K. *J. Am. Chem. Soc.* **2004**, *126*, 3321.

Replacement of gadolinium by an anisotropic lanthanide such as terbium preserves the tetranuclear nature of the products and allows them to function as single-molecule magnets. Indeed, the presence of a high-spin ground state and anisotropy are necessary to yield SMMs. This comparison underlines the importance of the anisotropy introduced here with help of the lanthanide ion to obtain convenient relaxation times. Unfortunately, our examples do not give an improvement of the SMM properties, in comparison to the example published previously.[14] A comparison of these results shows a possible role held by the auxiliary hfa ligands around the Tb ions because the main ligands are very similar. In the present work, we have focused our attention on disymmetric amide−imine ligands to find the ones capable of giving the best magnetic interactions in the tetranuclear species and to determine if some of them could give entities of higher nuclearity. This is why we have not used auxiliary ligands around the Ln centers. In a recent work, an alternative synthetic solution, making use of a trinuclear Cu−Ln−Cu entity with an amide function around each copper atom,[36] allowed us to isolate 1D Cu−Ln chains. We are now trying to obtain clusters of higher nuclearity via the introduction of two amide functions onto the same ligand. In a near future, we expect that the ligands described herein will allow us to introduce anisotropy with both ions, 3d and 4f.

(36) Costes, J. P.; Clemente-Juan, J. M.; Dahan, F.; Milon, J. *Inorg. Chem.* **2004**, *43*, 8200.

Acknowledgment. We thank Dr. A. Mari for his contribution to the magnetic measurements. This work was supported by the European Union sixth framework program NMP3-CT-2005-515767 entitled “MAGMANet: Molecular Approach to Nanomagnets and Multifunctional Materials”.

Supporting Information Available: X-ray crystallographic files in CIF format and further susceptibility and micro-SQUID measurements. This material is available free of charge via the Internet at http://pubs.acs.org.

IC050587O